Metabolomic and lipidomic landscape of porcine kidney associated with kidney perfusion in heart beating donors and donors after cardiac death

Iga Stryjak
Nicolaus Copernicus University
Natalia Warmuzińska
Nicolaus Copernicus University
Kamil Łuczykowski
Nicolaus Copernicus University
Peter Urbanellis
Toronto General Hospital
Markus Selzner
Toronto General Hospital
Barbara Bojko
bbojko@cm.umk.pl

Nicolaus Copernicus University

Article

Keywords: Solid-phase microextraction, SPME, LC-MS, kidney transplantation, metabolomics, lipidomics, graft quality assessment

Posted Date: August 16th, 2022

DOI: https://doi.org/10.21203/rs.3.rs-1948944/v1

Additional Declarations: No competing interests reported.

Version of Record: A version of this preprint was published at Translational Research on December 1st, 2023. See the published version at https://doi.org/10.1016/j.trsl.2023.12.001.

Abstract

With the ever-increasing shortage of kidney donors, transplant centers are faced with the challenge of finding ways to maximize their use of all available organ resources and extend the donor pool, including the use of expanded criteria donors. To address the need for a new analytical solution for graft quality assessments, we present a novel biochemical analysis method based on solid-phase microextraction (SPME) – a chemical biopsy. In this study, renal autotransplantation was performed in porcine models to simulate two types of donor scenarios: heart beating donors (HBD) and donors after cardiac death (DCD). All renal grafts were perfused using continuous normothermic ex vivo kidney perfusion. The small diameter of SPME probes enables minimally invasive and repeated sampling of the same tissue, thus allowing changes occurring in the organ to be tracked throughout the entire transplantation procedure. Samples were subjected to metabolomic and lipidomic profiling using high-performance liquid chromatography coupled with a mass spectrometer. As a result, we observed differences in the profiles of HBD and DCD kidneys. The most pronounced alterations were reflected in the levels of essential amino acids, purine nucleosides, lysophosphocholines, phosphoethanolamines, and triacylglycerols. Our findings demonstrate the potential of chemical biopsy in donor graft quality assessment and monitoring kidney function during perfusion.

1. Introduction

Kidney transplantation is a life-saving treatment for patients with end-stage renal dysfunction that enables higher survival rates and quality of life compared to dialysis treatment [1]. However, the number of patients placed on kidney transplant waiting lists is rapidly increasing, resulting in a growing gap between organ demand and availability. As a result, transplant centers are faced with the challenge of finding ways to maximize their use of all available organ resources and extend the donor pool in an attempt to close this gap [2][3]. Organs obtained from living donors offer several advantages for recipients, such as better graft function, faster recovery, and higher survival rates [4]. At the same time, it is more beneficial to obtain kidneys from expanded criteria donors (ECD) than to remain in a chronic dialysis program, especially in the case of elderly patients [3]. The use of kidneys from deceased donors whose heart has stopped beating—known as “donation after cardiac death” (DCD)—is a promising alternative approach with the potential to expand the donor pool. In contrast to live donations, DCD kidneys are exposed to warm ischemia time (WIT) during the period between cardiac arrest and graft preservation. This poses a challenge, as prolonged warm ischemia inevitably influences kidney allograft outcomes and can lead to delayed graft function (DGF) or primary nonfunction (PNF) [5][6]. An additional problem is the lack of reliable methods of assessing organ quality prior to transplantation. Currently, the surgeon decides whether to accept or decline a potential kidney based on their interpretation of the donor's recent laboratory tests and a visual evaluation of the organ. In some cases, a biopsy is used to evaluate tissue directly [2][7]. Although the biopsy procedure can yield significant information about pre-existing donor disease and vascular changes, it is not free of flaws. For example, the number of allowable biopsies during the transplantation procedure is strictly limited due to the procedure’s invasiveness, which

restricts its application for capturing dynamic changes and time-series analyses. While the value of histological findings is indisputable, they do not explain the molecular mechanisms of any observed aberrations [8]. Therefore, to increase the number of available organs for transplantation, a better method of assessing organ quality is direly needed.

Solid-phase microextraction (SPME) enables the detection of changes that occur in the organ during its preservation, spanning the period beginning with its removal from the donor's body and ending with its revascularization in the recipient's body [9]. The small diameter of the SPME probe (~ 200 µm) affords minimal invasiveness and allows the same organ to be sampled several times without damaging the tissue. Notably, SPME combines the sampling, extraction, and quenching of metabolites into a single step, making it a perfect tool for rapid on-site analysis. Furthermore, the biocompatibility of SPME coatings avoids the introduction of toxic compounds to the tissue and prevents the extraction of large molecules, such as proteins; as a result, enzymatic processes are already inhibited and the presence of artefacts are minimized at the time of sample collection, which is a great advantage over alternative sampling methods [10][11]. It is expected that the use of SPME will provide a more detailed understanding of the pre-transplant conditions responsible for delayed kidney function or dysfunction after transplantation, as well as how the graft preservation protocol influences the biochemistry of the organ.

Metabolomics and lipidomics have been recently recognized as promising approaches to attaining a better understanding of the changes in the biochemical pathways that occur during organ preservation [12][13][14]. Metabolomic and lipidomic profiling enable the monitoring of the system's immediate responses to sudden environmental changes related to organ removal, along with subsequent outcomes, such as ischemia, oxidative stress, or inflammatory responses [13][15][16][17]. Since the kidneys are largely associated with metabolic processes, measurements of metabolite and lipid concentrations may enable the identification of potential organ quality biomarkers, thus allowing better predictions regarding graft outcomes.

This preliminary study aims to demonstrate the SPME method's potential for evaluating kidney quality during the transplantation procedure, with particular emphasis on two types of donors: heart beating donors (HBD) and DCD. Moreover, the attempts were made to identify the set of metabolites of a potential diagnostic value for further investigation.

2. Materials And Methods

2.1. Chemicals

Pierce LTQ Velos ESI Positive External Calibrant Solution and Negative Ion Calibration Solution were purchased from Anchem (Anchem, Warsaw, Poland). Water (LC/MS Optima grade), ammonium acetate, formic acid, and acetic acid were purchased from Merck (Merck, Poznań, Poland), and acetonitrile, methanol, and isopropanol (all LC/MS Optima grade) were purchased form Alchem (Alchem, Torun,

Poland). Prototypes of biocompatible SPME mixed-mode probes (C18 and benzenesulfonic acid) were kindly provided by Supelco (Bellefonte, PA, USA).

2.2. Animal

Male Yorkshire pigs weighing 25–35 kg were used in this study. All animals received humane care in compliance with the “Principles of Laboratory Animal Care” formulated by the National Society for Medical Research and the “Guide for the Care of Laboratory Animals” published by the National Institutes of Health. All experimental protocols were approved by the Animal Care Committee at the Toronto General Hospital.

2.3. Solid-Phase Microextraction

Direct kidney sampling was conducted using SPME fibers coated with mixed-mode extraction phase to a length of 7 mm. Renal autotransplantation was performed in porcine models to simulate two types of donor scenarios: HBD and DCD (n = 3 in each group). Allocation of the animals to the given group was random. The samples were delivered to the laboratory and analyzed as blinded (labeled with numbers). All renal grafts were perfused using continuous normothermic *ex vivo* kidney perfusion (NEVKP). The autotransplantation procedure, warm ischemia induction, and NEVKP conditions are described elsewhere [18][19][20]. No additional inclusion/exclusion criteria were set. For both donor scenarios, sampling was performed *in vivo* before retrieval; after 1 h, 3 h, 5 h, and 7 h of perfusion; and again *in vivo* immediately after revascularization. In addition, kidneys from the DCD cases were also sampled after 45 min and 2 h of warm ischemia time (Fig. 1). Before sampling, all fibers were preconditioned for 60 min in a methanol/water (50:50 v/v) solution followed by rinsing with purified water for a few seconds. The extractions were performed by inserting the SPME fibers into the kidney cortex for 30 min at each time point. After sampling, the fibers were removed from the organ, quickly rinsed with water, and then gently dried with wipes to remove any tissue or blood residue. Next, the fibers were placed into empty glass vials and stored in a freezer at − 80 ∘C until analysis. All fibers were desorbed immediately before instrumental analysis. To this end, the SPME fibers were placed into vials containing 200 µL of desorption solution and agitated (1200 rpm) using a BenchMixer™ MultiTube Vortexer (Benchmark Scientific, Edison, USA) for 120 min. The compositions of the desorption solutions used in this work are described in [9]. To eliminate the analysis of contaminating compounds, extraction blanks were prepared. In this study, the extraction blanks consisted of fibers prepared using the same protocol as the rest of the fibers (preconditioning, desorption, etc.), only they were not used for kidney sampling.

2.4. Liquid Chromatography–High Resolution Mass Spectrometry Analysis (LC-HRMS)

Samples were analyzed using an LC-HRMS procedure based on the coupling of an ultra-high performance liquid chromatograph and a Q-Exactive Focus Orbitrap mass spectrometer. Data acquisition was performed using dedicated Thermo Scientific software, namely, Xcalibur 4.2 and Free Style 1.4 (Thermo Fisher Scientific, San Jose, California, USA). The instrument was calibrated via external

calibration every 72 h, resulting in a mass accuracy of < 2 ppm. Within-sequence samples were randomized, and pooled quality control (QC) samples composed of 10 µL of each sample were run every 8–10 injections to monitor instrument performance.

2.4.1. Metabolomic analysis

Chromatographic separation was carried out in reversed-phase (RP) using pentafluorophenyl column (Supelco Discovery HS F5, 2.1 mm × 100 mm, 3 µm) in positive and negative ionisation mode. The mobile phases were prepared according to the method detailed in [9]. The flow was set to 0.3 mL/min, and an injection volume of 10 µL was employed. The column temperature was set to 25 ◦C, and the sample vials were held at 4 ◦C in the autosampler. The mass spectrometer parameters in positive ionization mode were as follows: a sheath gas flow rate of 40 a.u.; an aux gas flow rate of 15 a.u.; a spray voltage of 1.5 kV; a capillary temp of 300 ◦C; an aux gas heater temp of 300 ◦C; an S-lens radio frequency level of 55%; an S-lens voltage of 25 V; and a skimmer voltage of 15 V. The scan range was set to *m/z* 80–1000 with a resolution of 70,000 full width at half maximum (FWHM). Acquisition was performed using an automatic gain control (AGC) target of 1E6, with the C-trap injection time set to auto. In negative ionization mode, the mass spectrometer parameters were as follows: a sheath gas flow rate of 48 a.u.; an aux gas flow rate of 11 a.u.; a spray voltage of 2.5 kV; a capillary temp of 256 ◦C; an aux gas heater temp of 413 ◦C; an S-lens radio frequency level of 55%; an S-lens voltage of -25 V; and a skimmer voltage of -15 V. In this mode, the scan range was set to *m/z* 80–1000 with a resolution of 70,000 FWHM. Acquisition was performed using an automatic gain control (AGC) target of 1E6, with the C-trap injection time set to auto.

The putative identification of compounds was confirmed based on Full MS/dd-MS2 mode. The fragmentation parameters were as follows: mass resolution—35,000 FWHM; AGC target—2E4; minimum AGC—8E3; intensity threshold—auto; maximum IT—auto; isolation window—3.0 *m/z*; stepped collision energy—10 V, 20 V, 40 V; loop count—2; and dynamic exclusion—auto.

2.4.2. Lipidomic analysis

Chromatographic separation was carried out on a hydrophilic stationary phase (HILIC) column (SeQuant ZIC-cHILIC, 3µm 100x2.1 mm) and in reversed-phase using a C18 column (Waters, XSelect CSH C18, 3.5µm, 2.1x75mm). The analyses were performed in positive electrospray ionization mode. The mobile phases were prepared using our previously published method [9]. A flow rate of 0.4 mL/min and a temperature of 40°C was used for the HILIC column, while a flow rate of 0.2 mL/min and temperature of 55°C was used for the RP column. The sample vials were held at 4°C in the autosampler, and an injection volume of 10µl was used. The mass spectrometer parameters for the HILIC separations were as follows: a spray voltage of 1500V; a capillary temperature of 325°C; sheath gas at 60 a.u.; an aux gas flow rate of 30 a.u.; a spare gas flow rate of 2 a.u.; a probe heater temperature of 325°C; an S-Lens radio frequency level of 55%; an S-lens voltage of 25 V; and a skimmer voltage of 15 V. For the RP analysis, the following HESI ion source parameters were employed: a spray voltage of 3500V; a capillary temperature of 275°C; sheath gas at 20 a.u.; an aux gas flow rate of 10 a.u.; a spare gas flow rate of 2 a.u.; a probe heater

temperature of 300°C; an S-Lens radio frequency level of 55%; an S-lens voltage of 25 V; and a skimmer voltage of 15 V. For both types of separation, the scan range was set to m/z 80-1000 with a resolution 70,000. In addition, in both cases, acquisition was performed using an AGC target of 1E6, and the C-trap injection time was set to auto.

The putative identification of compounds was confirmed based on Full MS/dd-MS2 mode using the following fragmentation parameters: mass resolution—35,000 full width at half maximum (FWHM); AGC target—2E4; minimum AGC—8E3; intensity threshold—auto; maximum IT—auto; isolation window—3.0 *m/z*; stepped collision energy—20 V, 30 V, 50 V; loop count—2; dynamic exclusion—auto.

2.5. Data Processing and Statistical Analysis

Metabolomic data processing was performed using Compound Discoverer 2.1. (Thermo Fisher Scientific, San Jose, California, USA) software with the following parameters: selected mass tolerance window—max 3 ppm; peak intensity > 10 000; signal-to-noise threshold > 3; and a max sample-to-blank ratio > 5. The QC-based area was used for correction (min 50% coverage, max 30% RSD in QC).

Features were putatively identified by searching for their exact molar weights in CEU Mass Mediator. The spectra of fragmented compounds were identified using Thermo Scientific FreeStyle 1.4 software linked to the mzCloud online database and by using MS/MS search in CEU Mass Mediator.

The lipidomic data was processed using LipidSearch 4.1.30 (Thermo Fisher Scientific, San Jose, California, USA) software with the following parameters: peak intensity > 10 000; a precursor tolerance of 5 ppm; a product tolerance of 10 ppm; an m-score threshold of 2; a Quan *m/z* tolerance of ± 5 ppm; a Quan RT (retention time) range of 0.5 min; use of main isomer filter. Protonated, sodiated, potassiated, and ammoniated adducts were considered for positive ion mode. After completing the lipid identification step, peak alignment was performed using the LipidSearch software and the following parameters: an m-Score threshold of 10; a retention time tolerance of 0.25 min; a QC-to-extraction blank ratio > 5; and a max 30% RSD in the QC.

The peak areas for the obtained compounds were analyzed using MetaboAnalyst 4.0 and Statistica 13.3 PL (StatSoft, Inc., Tulsa, Oklahoma, USA) software. All of the missing values were replaced with small values assumed to be a detection limit. Data were normalized by median, log-transformation, and Pareto scaling. A paired t-test was used to evaluate the statistical significance in normally distributed continuous parameters over time within the same group, while the Mann-Whitney U test was used to compare non-parametric variables. A P-value of < 0.05 was considered significant. In addition, principal component analysis (PCA) and partial least squares discriminant analysis (PLS-DA) were conducted to visually assess separation between sample groups, with variable importance in projection (VIP) scores > 1 being considered as significant. The PLS-DA model was cross-validated using leave-one-out cross validation. Two-dimensional score plots were generated to visually assess the separation of sample groups. A pattern matching method based on the *Pearson r* distance measure was implemented to search for

compounds with linearly changing relative concentrations over the time of perfusion and warm ischemia (across particular time points).

3. Results

Principal component analysis (PCA) was used to confirm the quality of the instrumental analysis. As shown in Figure S1 (A, B, C, D), the QC samples formed tight clusters, confirming the quality of the obtained results.

Particular time points were compared based on the experiment conditions (i.e., *in vivo* and *ex vivo* during perfusion), with the analysis of the results being divided into three categories: i) changes in the metabolomic and lipidomic profiles of the kidney during perfusion; ii) the influence of the whole transplantation procedure on HBD and DCD kidneys; and iii) comparison of the condition of the HBD and DCD grafts after the use of NEVKP. Lists of the identified metabolites and lipids are provided in Tables S1 and S2, respectively.

3.1. Evaluation of changes in kidney metabolomic and lipidomic profiles during normothermic *ex vivo* kidney perfusion.

The PLS-DA method was employed to obtain a more specific model of the differences in the metabolomic and lipidomic profiles of the HBD and DCD kidneys between perfusions (Fig. 2). Before constructing the PLS-DA models, separations of particular groups were evaluated on PCA scores plots (Figure S2). Each PLS-DA model was validated using leave-one-out cross validation. This statistical analysis allowed the number of features to be refined, yielding a set of compounds that differentiated the two analyzed groups. The differences observed within the metabolites in both positive and negative ionization modes were mainly related to a large group of amino acids and their derivatives. In terms of nucleosides, higher levels of adenosine and inosine were detected in the DCD grafts. The distinctions observed among lipids were mainly associated with phospholipids and triacylglycerols (TG) for the HILIC and RP separations, respectively. For instance, the DCD samples collected during perfusion contained higher levels of TG with carbon numbers (Cn) 30–40 compared to the corresponding HBD samples. Furthermore, the DCD samples were characterized by lower levels of lysophosphocholines (LPCs) compared to the HBD samples. Differences between levels of selected metabolites are shown in Fig. 3.

The Pearson correlation coefficient was used to evaluate changes across perfusion. The vast majority of the linearly correlated features were found in the metabolomic results rather than the lipidomic results. During perfusion, most of the compounds demonstrated a negative correlation with the HBD kidney, while no predominant trend was observed for the DCD graft. Boxplots of compounds that demonstrated linear correlations are shown in Fig. 4.

3.2. Influence of transplantation procedure on HBD and DCD kidneys

The two-dimensional score plots (PC1 vs. PC2) presented in Figures S3 and S4 illustrate the differences in the metabolomic and lipidomic patterns of the kidney cortex between consecutive stages of the transplantation procedure. Overlapping distributions can be observed for data points in the score plots for the donor kidney types and reperfusion, which may indicate similarities in their metabolic profiles. In each figure, the cluster linked to the perfusion is noticeably separated, as it refers to the *ex vivo* conditions (Figure S3 A, B, C, D). In contrast to the lipidome results (Figure S3 C, D), the metabolome of the kidney during warm ischemia time (Figure S3 A, B) is distinctly separated from other samples. Similarly, a slight overlapping of data points can be observed for HBD donor and reperfusion, as well as the separation of perfusion clusters (Figure S4 A, B, C, D). The overall trends in the levels of identified compounds are illustrated in the heat-maps shown in Figure S5.

A paired sample t-test was carried out to determine how the kidney's metabolic profile was affected by the autotransplantation procedure. Discriminative changes were mainly found in the lipidomic analyses. Among the identified lipids, the level of phosphoethanolamines (PEs) increased after the transplant procedure in the DCD grafts. In addition, decreased levels of LPCs, phosphocholines (PCs), and TG with Cn52 were also observed. Increased levels of TG with Cn30-40 were observed in the HBD kidneys, but no predominant trend for the relative concentrations of phospholipids before and after transplantation was detected. Changes in the levels of the selected metabolites are shown in Figure 5.

Moreover, the Pearson correlation coefficient was used to evaluate changes across warm ischemia time. The linear correlation of metabolites observed over warm ischemia time indicated dynamic changes within the organ involving positively correlated amino acids such as leucine, alanine, and valine ($r > 0,7$). Boxplots of compounds demonstrating linear correlation are shown in Fig. 6.

3.3. Comparison of the condition of HBD and DCD grafts after NEVKP

The Mann-Whitney U test was used to compare the condition of the HBD and DCD grafts after NEVKP. In addition, plots showing relative concentrations and time relationships were constructed to visualize the results and show trends among the compounds differentiating the perfusion and reperfusion time points (Fig. 7). In the metabolomic analysis, most of the compounds significantly differentiating the HBD and DCD kidneys after reperfusion were found to be present at higher levels in the DCD kidneys. These compounds included: alanine, glutamine, lysine, histidine, tryptophan, aspartic acid, cystine, adenosine, deoxyguanosine, inosine, pyroglutamic acid, and creatine. Conversely, higher levels of guanine, indolelactic acid, serine, valine, alpha-aminoadipic acid, and acetylcarnitine were observed in the HBD kidneys. In the lipidomic analysis, higher levels of PE P-34:4, PE P-36:5, TG 50:2, TG 52:3, and TG 52:2 were found in the HBD kidneys after perfusion, while higher levels of DG 32:0, TG 36:0, and TG 38:0 were found in the DCD kidneys after perfusion. Interestingly, an investigation of the plots showing relative

concentrations and time relationships revealed that 65% of the lipids and 44% of the other metabolites that differentiated perfusion in the PLS-DA models were present in relatively similar concentrations in the HBD and DCD kidneys after reperfusion.

4. Discussion

This study highlighted changes in the metabolomic and lipidomic profiles during renal autotransplantation. To the best of our knowledge, this work is the first to use SPME to compare two different types of kidney donors in a porcine autotransplantation model. The SPME probe's small size makes it possible to perform a chemical biopsy, which allows metabolites to be extracted directly from the organ without any tissue collection. The novelty of this work is its use of minimally invasive chemical biopsy to monitor the metabolomic and lipidomic profiles of kidneys via repeated sampling throughout the transplantation process.

In this study, alterations in purines and purine derivatives were observed for both the HBD and DCD groups. For the HBD kidneys, an overall decrease in hypoxanthine, adenosine, guanine, and inosine levels was observed after reperfusion, along with a corresponding increase in methyladenosine, deoxyguanosine, adenosine monophosphate (AMP), and allantoin. Similarly, a decrease in the concentration of hypoxanthine was observed in the DCD samples following reperfusion. However, in contrast to the HBD samples, the findings showed increased levels of inosine and adenosine, as well as a decline in methyladenosine, deoxyguanosine, and allantoin in the DCD kidneys after transplantation. Furthermore, we observed an increase in hypoxanthine, deoxyguanosine, and methyladenosine, and the downregulation of inosine levels in the DCD samples during warm ischemia time. Moreover, a comparison of the DCD and HBD grafts during perfusion revealed higher concentrations of adenosine, inosine, and deoxyguanosine in the DCD samples. It has been previously hypothesized that, as breakdown products od adenosine triphosphate (ATP), purines play an important role in the molecular mechanisms of ischemia and hypoxia. The oxidation of hypoxanthine is disturbed during ischemia and hypoxia, causing the accumulation of hypoxanthine in the cells. Once the ischemic tissue is re-supplied with blood, the molecular oxygen catalyses hypoxanthine conversion by xanthine oxidase, liberating reactive oxygen species (ROS) [21]. Wijermars et al. assessed the accumulation of hypoxanthine during warm ischemia stimulated in kidney biopsies [22]. In a separate study, Fujii et al. found elevated hypoxanthine levels in every region of mural kidneys subjected to the 10 minutes of ischemia [23]. These results are consistent with the findings of the present work, which detected higher levels of hypoxanthine during warm ischemia time. Elsewhere, Hayashi et al. observed elevated levels of serum hypoxanthine in patients with stage 1–2 chronic kidney disease (CKD). It is important to note that hypoxanthine can act as a cardiotoxin due to its possible involvement in mitochondrial degradation during oxidative stress, which can contribute to the increased frequency of cardiovascular incidents [24]. The findings of numerous studies suggest the significant role of adenosine in controlling cellular adaptation to hypoxia, ischemia, and inflammatory processes, as well as its protective role in preventing ischemia-reperfusion injury. Such conditions wherein oxygen supply is limited are related to intensified extracellular adenosine production due to the associated breakdown of ATP and adenosine diphosphate (ADP) [25][26][27][28]

[29]. Our findings showed that adenosine and urocanic acid were the only metabolites to demonstrate significant linear progressive accumulation during the perfusion of HBD kidneys. Previous reports have well-established the role of adenosine accumulation and the activation of its four receptor subtypes (A_1AR, A_{2A}AR, A_{2B}AR, and A_3AR) in protecting organs from ischemia-reperfusion injury [23][28]. Inosine is a breakdown product of adenosine nucleotides, such as ATP, ADP, and AMP. Previous studies focusing on renal DCD allografts have found significantly lower levels of inosine in the perfusate from kidneys with DGF compared to the perfusate from immediate graft function (IGF) during hypothermic machine perfusion (HMP) [30][31]. Surprisingly, this reduction was noticed in the DGF grafts, which are more ischemicaly affected compared to IGF grafts. Similarly, our comparison of HBD and DCD kidneys during perfusion indicated significantly lower concentrations of inosine in DCD grafts subjected to warm ischemia.

A thorough analysis of kidney graft tissue revealed that amino acid pathways were the most modulated. We observed significant linear growth of alanine, leucine, and valine concentrations during *in vivo* warm ischemia progression in DCD kidneys, as well as the accumulation of these amino acids in both HBD and DCD kidneys during perfusion. Interestingly, during perfusion, significantly higher levels of valine were found in HBD kidneys, while higher levels of alanine were detected in DCD kidneys. Numerous previous reports suggest the involvement of alanine, valine and, to a lesser extent, leucine in the impairment of organ function. Liu et al.'s findings suggest that alanine is a sensitive discriminator of warm ischemia during porcine liver HMP [32], while Bruinsma et al. observed elevated levels of alanine and valine during sub-normothermic machine perfusion of DCD human livers [33]. Elsewhere, Bon et al. found that increased concentrations of alanine and valine in perfused kidneys tended to result in less favourable outcomes [34]. It has also been noted that increased urinary valine and alanine concentrations are associated with renal cortical damage [35]. Additionally, significantly higher levels of alanine and leucine were detected in the perfusate of DGF kidneys, which may be associated with cellular damage that occurs after the release of protein breakdown products into the perfusate [30].

In the present study, a significant linear relationship between concentration and perfusion time was observed for several compounds. Linear reductions in serine and phenylalanine levels were noted for the HBD kidneys, while in the DCD kidneys, linear reductions in histidine levels were detected. In contrast, significant linear growth in lysine and methionine sulfoxide levels was observed for the DCD grafts. Moreover, decreases in phenylalanine, histidine, and methionine sulfoxide levels were observed during warm ischemia time. Previous reports have indicated that phenylalanine levels decrease as kidney function impairment progresses, which, may complement our findings related to the downregulation of this amino acid during perfusion [36]. Furthermore, the alleviation of plasma and perfusate phenylalanine levels has been associated with rapid CKD development and DGF, respectively [31][37]. Zhang et al. reported a significant decrease in phenylalanine and histidine levels in the urine of rats with CKD, indicating the possible impairment of these amino acids or intensified catabolism [38]. These findings are supported by those of another study, which showed a significant relationship between low levels of plasma histidine and greater mortality in CKD patients [39]. It has been hypothesized that reduced

histidine concentrations are related to protein-energy wasting, systemic inflammatory processes, and oxidative stress development. Histidine is thought to act as an anti-oxidant agent due to its ability to scavenge the ROS generated by cells during inflammation [39][38]. In addition, urinary histidine levels were lower in patients with impaired graft function after renal transplantation compared to those with well-preserved renal function [40]. Our data revealed a significant linear increase in methionine sulfoxide concentrations throughout the time of preservation for DCD patients. It has been recently established that the cyclic oxidation of methionine to methionine sulfoxide and its subsequent reduction back to methionine is an important protective mechanism against reactive oxygen species. It is believed that the severity of changes in post-ischemic histological kidneys is correlated with methionine sulfoxide reductase A. The accumulation of methionine sulfoxide in renal tissue during the preservation of kidneys may be associated with the ongoing progression of oxidative stress [24][41].

Lipids play a fundamental role in biological systems, including intracellular and intercellular signalling, energy storage, and membrane bilayer structure [42][16]. Phospholipids account for more than 50% of the total lipid concentration in a normal human kidney, while triglycerides make up 20% and free non-esterified fatty acids (FA) comprise 10%. Notably, lipids appear to be potential markers of kidney disease and injury [42], as our results showed changes in the concentrations of glycerolipids and phospholipids in the kidney cortex during transplantation. In the DCD and HBD groups, relevant changes in LPCs levels were observed following reperfusion. For instance, reduced levels of LPC 18:0 were detected in both the HBD and DCD kidneys. In addition, levels of LPC 20:4 were lower than the baseline for both donor types, but this reduction was only significant for the DCD kidneys. Similarly, while increased levels of LPC P-16:0 were observed in both donor types, this increase was only significant in the HBD grafts. Moreover, we observed a non-significant elevation in the overall levels of LPCs during warm ischemia. LPCs are generated from phosphatidylcholine via the action of phospholipase A2 (PLA2) and/or by the transfer of FA to free cholesterol via lecithin-cholesterol acyltransferase (LCAT). LPCs, via G protein-coupled receptors and Toll-like receptors, activate multiple signalling pathways and may have harmful effects on various cells, including increasing oxidative stress and enhancing inflammatory responses [43][44]. However, recent studies have been inconclusive, and the mechanisms underlying the harmful effects of LPCs have not been fully investigated and are not well-understood [43]. Rao et al. observed a significant increase in LPC 18:0 and decreases in LPC 20:0 and LPC 20:4 24h after ischemia/reperfusion-induced acute kidney injury in a mouse model. [15]. Elsewhere, Solati et al. reported a significant increase in LPC 22:5 and non-significant increases in other LPC species after 6h ischemia/reperfusion (I/R) in a rat model. Interestingly, levels of these LPCs normalized after 24h [45]. In other work, Chen et al. observed increased levels of LPC 24:1 in patients with stage 4 and 5 CKD [46], while Xu et al. detected higher levels of LPC 16:0 and LPC 18:0 in DCD livers at the pre-transplantation stage. In the latter study, the biopsy was taken at the end of cold preservation before implantation; however, the LPCs in question were detected at lower concentrations following reperfusion [44]. These results are consistent with those of the present work, which found that LPCs levels may increase during warm ischemia and decrease after reperfusion. In the current study, LPC P-16:0 was the only LPC that increased after reperfusion. Additionally, a comparison of the HBD and DCD grafts during perfusion showed lower levels of numerous

LPCs in the DCD kidneys, including LPC 16:1, LPC 18:1, LPC 20:4, LPC P-16:0, and LPC 18:0. Rhee et al. have reported declining levels of LPCs, including LPC 18:1 and LPC 18:0, in patients with CKD and declining levels of LPC 14:0 in patients with end-stage renal disease [47][48]. Furthermore, Tsai et al. have recently shown lower levels of LPC 16:0 in recipients with early allograft dysfunction (EAD) compared to those in a non-EAD group on day 7 post-operation. In this lipidomic analysis, blood acquired from 51 recipients undergoing living-donor liver transplantation was evaluated [49]. LPCs with a single acyl chain are breakdown products of membrane phospholipids; hence, previous findings have suggested that a reduction in LPCs indicates that membrane breakdown and remodelling might be transiently inhibited following ischemia/reperfusion [50].

PCs and PEs are the most abundant phospholipids in all mammalian cell and subcellular organelles. While previous research suggests that an alteration in the absolute concentrations of these phospholipids is not a key determinant of cellular processes associated with health and disease, the PC/PE ratio may be [51]. In this work, we observed a significant reduction in PC 36:3 in the DCD kidneys after reperfusion. Rao et al. and Solati et al. have reported elevated levels of PCs in mice and rat I/R models. Similar to the results presented herein, Chen et al. observed a decrease in PC 20:2 and PC 24:1 in patients with stage 4 and 5 CKD [48]. In addition, previous studies have also reported reduced levels of PC 34:4, PC 32:2, and PC 38:3 in patients with end-stage renal disease [47]. Interestingly, in the DCD group, we observed significant increases in PE O-38:6, PE O-38:5, and PE 36:2 after reperfusion, and non-significant increases in other identified PEs. Despite a non-significant elevation in the overall levels of PEs in the HBD group following reperfusion, we observed a significant increase in PE 36:2 compared to the baseline. In addition, the HBD group showed higher levels of PE P-34:4 and PE P-36:5 compared to the DCD group following reperfusion. Rao et al. documented reduced PE levels in a mouse model of renal I/R after 6h and 24h reperfusion [15], and Solati et al. similarly observed significant decreases in PE levels in a rat model of renal I/R [45]. In the present study, we observed reduction of PEs after warm ischemia and an increase after reperfusion (Figure S5 E). This trend was also observed by Afshinnia et al., who also found similar elevations in the abundance of PEs in 5 stage CKD patients. In this lipidomic analysis, increased levels of polyunsaturated lipids with higher numbers of double bonds were associated with progressive CKD [52]. Moreover, recent findings have suggested that higher levels of PEs are associated with a higher risk of diabetic kidney disease progression [53]. PEs are multifunctional lipids that play an essential role in various cellular processes, including serving as a substrate for post-translational modification; promoting organelle, cell, and membrane fusion; oxidative phosphorylation; and mitochondrial biogenesis [51][53][54]. However, the mechanism linking PEs and kidney disease progression is not well understood and remains unidentified. In the current study, elevated levels of several PEs and reduced levels of PC 36:4 and PC 36:3 in DCD kidneys were observed. These alterations may impact the overall PC/PE ratio, which can in turn influence processes in a number of organelles. For instance, a lower PC/PE ratio may impair liver regeneration, affect energy metabolism, increase cell leakage, and cause endoplasmic reticulum stress [51].

Another of the present study's notable findings was alterations in neutral glycerolipids, including TG and DG. In the DCD grafts, significant reductions in DG 34:1, TG 52:1, TG 52:4, TG 52:3, and TG 52:2 were

observed following reperfusion. By comparison, significant elevations in TG 38:0, TG 40:0, TG 36:0, TG 34:0, and TG 32:0 were observed in the HBD kidneys. Moreover, a comparison of the HBD and DCD groups during perfusion revealed higher levels of TG with Cn30-40, including TG 30:0, TG 32:0, TG 34:0, TG 36:0, TG 38:0, and TG 40:0, in the DCD samples. Since the main function of triacylglycerols is fat storage, they provide an efficient mechanism for the storing fatty acids. The metabolism of TGs provides precursors (fatty acids and diacylglycerol) for membrane-lipid synthesis [55]. Elevated TG levels have been previously reported in acute kidney injury and CKD studies, but most of this research has mainly measured total TG levels. Recent lipidomic studies have found that the number of polyunsaturated TGs with higher carbon numbers increases between stage 2 and stage 5 of CKD, while the number of TGs with the low carbon numbers and low numbers of double bonds decreases [46][52]. Similarly, Afshinnia et al. reported higher levels of longer TGs with more double bonds and lower levels of shorter TGs with fewer double bonds in people with DKD progression [53]. The renal toxicity of TGs depends on their acyl length and the number of double bonds, and the accumulation of neutral lipids in the cell is usually associated with lipotoxicity [53][56]. However, TGs are a reservoir for excess free fatty acids that have been removed from cells, thus preventing fatty-acid-induced lipotoxicity. Overall, the main renal toxicities are related to saturated fatty acids that, for example, can promote mitochondrial superoxide generation and endoplasmic reticulum stress. Since TGs are less toxic than nonesterified saturated fatty acids [53][56][57], a higher abundance of saturated TGs with relatively shorter acyl chains may reflect an adaptive mechanism for detoxifying toxic saturated fatty acids. However, lipid accumulation may be either protective or toxic depending on the time course of I/R and the duration of lipid overload. Previous metabolomics studies have reported elevated glycerol levels at early ischemia reperfusion injury (IRI) time points, suggesting TGs lipolysis as a source of free FAs. Exceeding cellular capacity for TG storage or hydrolysis could theoretically cause lipid-induced cell dysfunction or death, including via protein acylation, altered mitochondrial energy coupling, cell membrane damage, the release of pro-inflammatory/pro-apoptotic factors, increased cellular oxidative stress, and endoplasmic reticulum [57].

Additionally, in both the metabolomic and lipidomic analyses, the compounds that differentiated perfusion in PLS-DA models were observed in similar relative concentrations for the HBD and DCD kidneys after reperfusion. This finding suggests that NEVKP may have a positive influence on kidney graft quality. NEVKP is a novel technology for graft preservation that is capable of providing near-physiological conditions, with the findings of several preclinical studies having suggested its superiority over static cold storage (SCS), especially for DCD kidneys. NEVKP may reduce cold ischemia time and mitigate the harmful effect of I/R injury [58]. Previous studies have found that kidneys subjected to NEVKP exhibit faster functional recovery compared to those subjected to SCS. Furthermore, findings indicate that NEVKP might protect against graft injury and improve marginal graft function, which may help increase the donor pool [59][60][61]. Indeed, coupled with previous reports, the findings of the present study suggest that NEVKP technology is potentially a superior kidney-preservation strategy.

Despite these promising results, this study has several limitations. First, our metabolomic and lipidomic approaches were based on untargeted data collection; therefore, the concentrations of compounds are given as relative, normalized amounts. However, the similarity of our results to those of previous studies

indicates the validity of our platform. Furthermore, we acknowledge that complex lipids may include several isomers with various acyl chains and saturation statuses, and that a variety of different isomers can be present for any given lipid feature. In addition, traditional UHPLC-HRMS/MS does not provide information about the double bond position, orientation, or stereochemistry [62]. Hence, in this study, we annotated lipids by class and the sum composition of carbons and double bonds in the lipid fatty acyl chains. It is also important to emphasize that future studies should compare these results with routinely assessed clinical parameters to provide a comprehensive evaluation of the proposed method and its usefulness in graft quality assessment. Another limitation was the small sample sizes. However, this was consistent with the 3R principles (Replacement, Reduction, and Refinement) guiding animal experimentation, which call for the use of as few animals as possible [63]. Moreover, the use of SPME enables multiple analyses over time, which increased the number of samples that can be taken without requiring more animals. Based on the acquired samples, we validated the PLS-DA models and identified relevant metabolites that may have future diagnostic meaning.

5. Conclusion

In summary, SPME followed by LC-MS/MS analysis permits the sampling of biological matrices and the capture and detection of numerous compounds with different polarities. Additionally, the small diameter of SPME probes enables minimally invasive and repeated sampling of the same tissue, thus allowing changes occurring in the organ to be tracked throughout the entire transplantation procedure—from graft collection, through organ storage, to reperfusion. As a result, we were able to observe differences in the metabolomic and lipidomic profiles of HBD and DCD kidneys. The most pronounced alterations were reflected in the levels of essential amino acids, purine nucleosides, LPCs, PEs and TGs. However, future quantitative targeted studies are required to validate the current findings and to evaluate the predictive value of the selected metabolites.

Abbreviations

ADP adenosine diphosphate; AMP adenosine monophosphate; ATP adenosine triphosphate; CAR acyl carnitine; CE cholesterol ester; CKD chronic kidney disease; Cn carbon numbers; DCD donor after cardiac death; DG diglyceride; DGF delayed graft function primary nonfunction; DKD diabetic kidney disease; EAD early allograft dysfunction; ECD expanded criteria donor; FA fatty acid; HBD heart beating donor; HILIC hydrophilic interaction liquid chromatography; HMP hypothermic machine perfusion; IGF immediate graft function; I/R ischemia/ reperfusion; IRI ischemia reperfusion injury; LPC lysophosphocholine; MG monoglyceride; NEVKP normothermic ex vivo kidney perfusion; PC phosphocholine; PCA principal component analysis; PE phosphoethanolamine; PLS-DA partial least squares discriminant analysis; PNF primary nonfunction; QC quality control; ROS reactive oxygen species; RP reversed-phase chromatography; SM sphingomyelin; SPME solid phase microextraction; TG triacylglycerol; VIP The Variable Importance in Projection; WIT warm ischemia time

Declarations

Acknowledgments

The study is reported in accordance with ARRIVE guidelines; details of the chemical biopsy protocols are described in Materials and Methods section of this manuscript, while information of animal handling and surgical procedures can be found in [18-20]. This study was funded by National Science Centre, grant Opus No. 2017/27/B/NZ5/01013. The authors would like to acknowledge Supelco/MilliporeSigma for kindly supplying the SPME probes and Thermo Fisher Scientific for granting us access to a Q-Exactive Focus mass spectrometer. BB would like to thank Prof. Janusz Pawliszyn for arranging the opportunity to collect the samples used in this work at the Toronto General Hospital during her stay at the University of Waterloo.

Author Contributions

Conceptualization: B.B., M.S.; methodology: I.S., N.W., P.U., M.S., B.B.; samples collection: P.U., M.S.; formal analysis: I.S., N.W., K.Ł.; investigation: I.S., N.W., K.Ł., B.B.; resources: B.B.,M.S.; data curation: I.S., N.W.; writing—original draft preparation: I.S., N.W.; writing—review and editing, I.S., N.W., B.B., M.S.; visualization, N.W; supervision: B.B; funding acquisition: B.B.

Data availability statement

The datasets generated during and/or analysed during the current study are available from the corresponding author on reasonable request.

Competing interests

The authors declare no competing interests.

References

1. Swanson, K. J. *et al.* Role of novel biomarkers in kidney transplantation. World J. Transplant. **10**, 230–255 (2020).
2. Moeckli, B. *et al.* Evaluation of donor kidneys prior to transplantation: an update of current and emerging methods. Transpl. Int. **32**, 459–469 (2019).
3. Filiopoulos, V. & Boletis, J. N. Renal transplantation with expanded criteria donors: Which is the optimal immunosuppression? World J. Transplant. **6**, 103 (2016).
4. Bellini, M. I., Courtney, A. & McCaughan, J. Living Donor Kidney Transplantation Improves Graft and Recipient Survival in Patients with Multiple Kidney Transplants. J. Clin. Med. **9**, 2118 (2020).
5. Peters-Sengers, H. *et al.* Impact of Cold Ischemia Time on Outcomes of Deceased Donor Kidney Transplantation: An Analysis of a National Registry. Transplant. Direct **5**, 1–11 (2019).

6. Bellini, M. I., Nozdrin, M., Yiu, J. & Papalois, V. Machine Perfusion for Abdominal Organ Preservation: A Systematic Review of Kidney and Liver Human Grafts. J. Clin. Med. **8**, 1221 (2019).
7. Dare, A. J., Pettigrew, G. J. & Saeb-Parsy, K. Preoperative assessment of the deceased-donor kidney: From macroscopic appearance to molecular biomarkers. Transplantation **97**, 797–807 (2014).
8. Plattner, B. W. *et al.* Complications and adequacy of transplant kidney biopsies: A comparison of techniques. J. Vasc. Access **19**, 291–296 (2018).
9. Stryjak, I. *et al.* Using a chemical biopsy for graft quality assessment. J. Vis. Exp. e60946 (2020). doi:10.3791/60946
10. Reyes-Garcés, N. *et al.* Advances in Solid Phase Microextraction and Perspective on Future Directions. Anal. Chem. **90**, 302–360 (2018).
11. Filipiak, W. & Bojko, B. SPME in clinical, pharmaceutical, and biotechnological research – How far are we from daily practice? TrAC - Trends Anal. Chem. **115**, 203–213 (2019).
12. Kvietkauskas, M. *et al.* The role of metabolomics in current concepts of organ preservation. Int. J. Mol. Sci. **21**, 1–17 (2020).
13. Stryjak, I., Warmuzińska, N., Bogusiewicz, J., Łuczykowski, K. & Bojko, B. Monitoring of the influence of long-term oxidative stress and ischemia on the condition of kidneys using solid-phase microextraction chemical biopsy coupled with liquid chromatography–high-resolution mass spectrometry. J. Sep. Sci. **43**, 1867–1878 (2020).
14. Raigani, S. *et al.* Metabolic and lipidomic profiling of steatotic human livers during ex situ normothermic machine perfusion guides resuscitation strategies. PLoS One **15**, 1–20 (2020).
15. Rao, S. *et al.* Early lipid changes in acute kidney injury using SWATH lipidomics coupled with MALDI tissue imaging. Am. J. Physiol. - Ren. Physiol. **310**, F1136–F1147 (2016).
16. Afshinnia, F. *et al.* Lipidomics and Biomarker Discovery in Kidney Disease. Semin. Nephrol. **38**, 127–141 (2018).
17. Abbiss, H., Maker, G. L. & Trengove, R. D. Metabolomics approaches for the diagnosis and understanding of kidney diseases. Metabolites **9**, (2019).
18. Kaths, J. M. *et al.* Normothermic ex vivo kidney perfusion for the preservation of kidney grafts prior to transplantation. J. Vis. Exp. **2015**, 1–13 (2015).
19. Kaths, J. M. *et al.* Heterotopic renal autotransplantation in a porcine model: A step-by-step protocol. *J. Vis. Exp.* 2016, 1–9 (2016).
20. Kaths, J. M. *et al.* Normothermic ex vivo kidney perfusion for graft quality assessment prior to transplantation. Am. J. Transplant. **18**, 580–589 (2018).
21. Prieto-Moure, B. *et al.* Allopurinol in renal ischemia. Journal of Investigative Surgery **27**, 304–316 (2014).
22. Wijermars, L. G. M. *et al.* Defective postreperfusion metabolic recovery directly associates with incident delayed graft function. Kidney Int. **90**, 181–191 (2016).

23. Fujii, K. *et al.* Xanthine oxidase inhibitor ameliorates postischemic renal injury in mice by promoting resynthesis of adenine nucleotides. JCI Insight **4**, 1–20 (2019).
24. Hayashi, K. *et al.* Use of serum and urine metabolome analysis for the detection of metabolic changes in patients with stage 1–2 chronic kidney disease. Nephrourol. Mon. **3**, 164–171 (2011).
25. Rabadi, M. M. & Lee, T. H. Adenosine Receptors and Renal Ischemia Reperfusion Injury. Acta Physiol. **213**, 222–231 (2015).
26. Bauerle, J. D., Grenz, A., Kim, J. H., Lee, H. T. & Eltzschig, H. K. Adenosine generation and signaling during acute kidney injury. J. Am. Soc. Nephrol. **22**, 14–20 (2011).
27. Zimmerman, M. A., Kam, I., Eltzschig, H. & Grenz, A. Biological implications of extracellular adenosine in hepatic ischemia and reperfusion injury. Am. J. Transplant. **13**, 2524–2529 (2013).
28. Han, S. J. & Thomas Lee, H. Mechanisms and therapeutic targets of ischemic acute kidney injury. Kidney Res. Clin. Pract. **38**, 427–440 (2019).
29. Fisher, O., Benson, R. A. & Imray, C. H. The clinical application of purine nucleosides as biomarkers of tissue Ischemia and hypoxia in humans in vivo. Biomark. Med. **13**, 953–965 (2018).
30. Guy, A. J. *et al.* Metabolomic analysis of perfusate during hypothermic machine perfusion of human cadaveric kidneys. Transplantation **99**, 754–759 (2015).
31. Wang, Z. *et al.* Proton nuclear magnetic resonance (1H-NMR)-based metabolomic evaluation of human renal allografts from donations after circulatory death. Med. Sci. Monit. **23**, 5472–5479 (2017).
32. Liu, Q. *et al.* Discriminate Liver Warm Ischemic Injury During Hypothermic Machine Perfusion by Proton Magnetic Resonance Spectroscopy: A Study in a Porcine Model. *Transplant. Proc.* **41**, 3383–3386 (2009).
33. Bruinsma, B. G. *et al.* Metabolic profiling during ex vivo machine perfusion of the human liver. Sci. Rep. **6**, 1–13 (2016).
34. Bon, D. *et al.* Analysis of perfusates during hypothermic machine perfusion by NMR spectroscopy: A potential tool for predicting kidney graft outcome. Transplantation **97**, 810–816 (2014).
35. Wishart, D. S. Metabolomics in monitoring kidney transplants. Curr. Opin. Nephrol. Hypertens. **15**, 637–642 (2006).
36. Li, R., Dai, J. & Kang, H. The construction of a panel of serum amino acids for the identification of early chronic kidney disease patients. J. Clin. Lab. Anal. **32**, 1–7 (2018).
37. Rhee, E. P. *et al.* Metabolomics of Chronic Kidney Disease Progression: A Case-Control Analysis in the Chronic Renal Insufficiency Cohort Study. Am. J. Nephrol. **43**, 366–374 (2016).
38. Zhang, Z. H. *et al.* Metabolomics insights into chronic kidney disease and modulatory effect of rhubarb against tubulointerstitial fibrosis. Sci. Rep. **5**, 1–17 (2015).
39. Watanabe, M. *et al.* Consequences of low plasma histidine in chronic kidney disease patients: Associations with inflammation, oxidative stress, and mortality. Am. J. Clin. Nutr. **87**, 1860–1866 (2008).

40. Bassi, R. *et al.* Metabolomic profiling in individuals with a failing kidney allograft. PLoS One **12**, 1–14 (2017).
41. Tolun, A. A. *et al.* Allantoin in Human Urine Quantified by UPLC-MS/MS. Anal Biochem **402**, 191–193 (2010).
42. Zhao, Y. Y., Vaziri, N. D. & Lin, R. C. *Lipidomics: New insight into kidney disease*. *Advances in Clinical Chemistry* **68**, (Elsevier Inc., 2015).
43. Law, S. *et al.* An Updated Review of Lysophosphatidylcholine Metabolism in Human Diseases. **2**, 1–24 (2019).
44. Xu, J. *et al.* Lipidomics comparing DCD and DBD liver allografts uncovers lysophospholipids elevated in recipients undergoing early allograft dysfunction. Sci. Rep. **5**, 1–10 (2015).
45. Solati, Z., Edel, A. L., Shang, Y., Karmin, O. & Ravandi, A. Oxidized phosphatidylcholines are produced in renal ischemia reperfusion injury. PLoS One **13**, e0195172 (2018).
46. Chen, H., Chen, L., Liu, D., Chen, D. & Vaziri, N. D. Article A combined clinical phenotype and lipidomic analysis reveals the impact of chronic kidney disease on lipid metabolism. (2017). doi:10.1021/acs.jproteome.6b00956
47. Rhee, E. P. *et al.* Metabolite profiling identifies markers of uremia. J. Am. Soc. Nephrol. **21**, 1041–1051 (2010).
48. Rhee, E. P. *et al.* A combined epidemiologic and metabolomic approach improves CKD prediction. J. Am. Soc. Nephrol. **24**, 1330–1338 (2013).
49. Tsai, H.-I. *et al.* A Lipidomics Study Reveals Lipid Signatures Associated with Early Allograft Dysfunction in Living Donor Liver Transplantation. J. Clin. Med. **8**, 30 (2018).
50. Wei, Q., Xiao, X., Fogle, P. & Dong, Z. Changes in metabolic profiles during acute kidney injury and recovery following ischemia/reperfusion. PLoS One **9**, 1–13 (2014).
51. van der Veen, J. N. *et al.* The critical role of phosphatidylcholine and phosphatidylethanolamine metabolism in health and disease. Biochim. Biophys. Acta - Biomembr. **1859**, 1558–1572 (2017).
52. Afshinnia, F. *et al.* Impaired b -Oxidation and Altered Complex Lipid Fatty Acid Partitioning with Advancing CKD. 1–12 (2017). doi:10.1681/ASN.2017030350
53. Afshinnia, F. *et al.* Increased lipogenesis and impaired B-oxidation predict type 2 diabetic kidney disease progression in American Indians. JCI Insight **4**, 1–19 (2019).
54. Calzada, E., Onguka, O. & Claypool, S. M. Phosphatidylethanolamine Metabolism in Health and Disease. Int. Rev. Cell Mol. Biol. **321**, 29–88 (2016).
55. Process, A. *Encyclopedia of Biophysics*. *Encyclopedia of Biophysics* (2013). doi:10.1007/978-3-642-16712-6
56. Weinberg, J. M. Lipotoxicity. Kidney Int. **70**, 1560–1566 (2006).
57. Erpicum, P., Rowart, P., Defraigne, J. O., Krzesinski, J. M. & Jouret, F. What we need to know about lipid-associated injury in case of renal ischemia-reperfusion. Am. J. Physiol. - Ren. Physiol. **315**, F1714–F1719 (2018).

58. Hamelink, T. L. *et al.* Renal Normothermic Machine Perfusion: The Road Toward Clinical Implementation of a Promising Pretransplant Organ Assessment Tool. Transplantation **106**, 268–279 (2022).
59. Kaths, J. M. *et al.* Continuous Normothermic Ex Vivo Kidney Perfusion Is Superior to Brief Normothermic Perfusion Following Static Cold Storage in Donation After Circulatory Death Pig Kidney Transplantation. Am. J. Transplant. **17**, 957–969 (2017).
60. Kaths, J. M. *et al.* Continuous Normothermic Ex Vivo Kidney Perfusion Improves Graft Function in Donation after Circulatory Death Pig Kidney Transplantation. Transplantation **101**, 754–763 (2017).
61. Urbanellis, P. *et al.* Normothermic Ex Vivo Kidney Perfusion Improves Early DCD Graft Function Compared with Hypothermic Machine Perfusion and Static Cold Storage. *Transplantation* 947–955 (2020). doi:10.1097/TP.0000000000003066
62. Koelmel, J. P., Ulmer, C. Z., Jones, C. M., Yost, R. A. & Bowden, J. A. Common cases of improper lipid annotation using high-resolution tandem mass spectrometry data and corresponding limitations in biological interpretation. Biochim. Biophys. Acta - Mol. Cell Biol. Lipids **1862**, 766–770 (2017).
63. National Centre for the Replacement, Refinement and Reduction of Animals in Research https://nc3rs.org.uk/who-we-are/3rs last accessed: 25 July 2022.

Figures

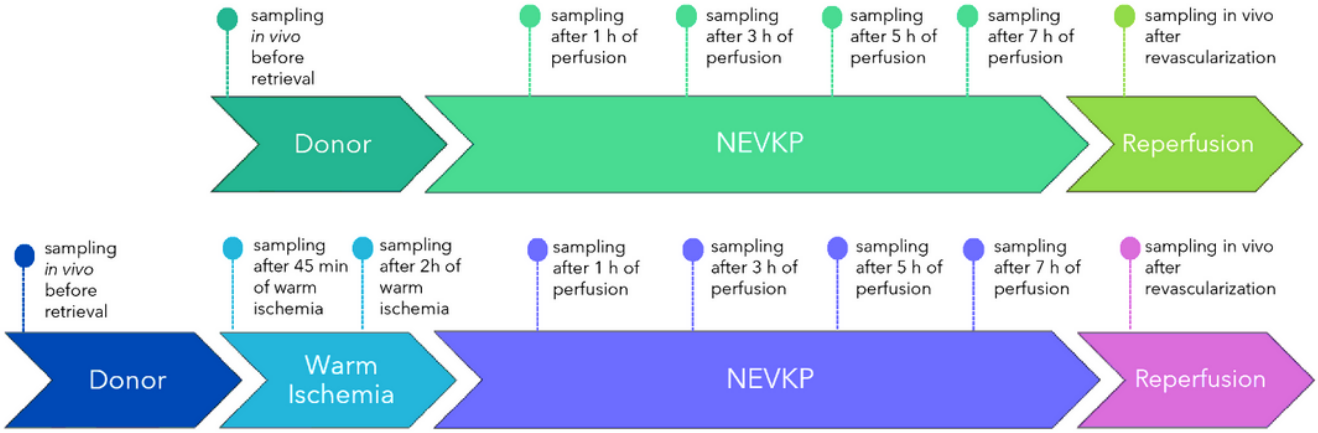

Figure 1

Study design. Two types of donor scenarios—heart beating donors (HBD) and donors after cardiac death (DCD)—were examined in porcine models of renal autotransplantation. All renal grafts were perfused at 37°C with the use of continuous normothermic *ex vivo* kidney perfusion (NEVKP). Sampling was performed as follows: *in vivo* before retrieval; after 1 h, 3 h, 5 h, 7 h of perfusion; and *in vivo* immediately

after revascularization. In addition, the DCD kidneys were also sampled after 45 min and 2 h of warm ischemia.

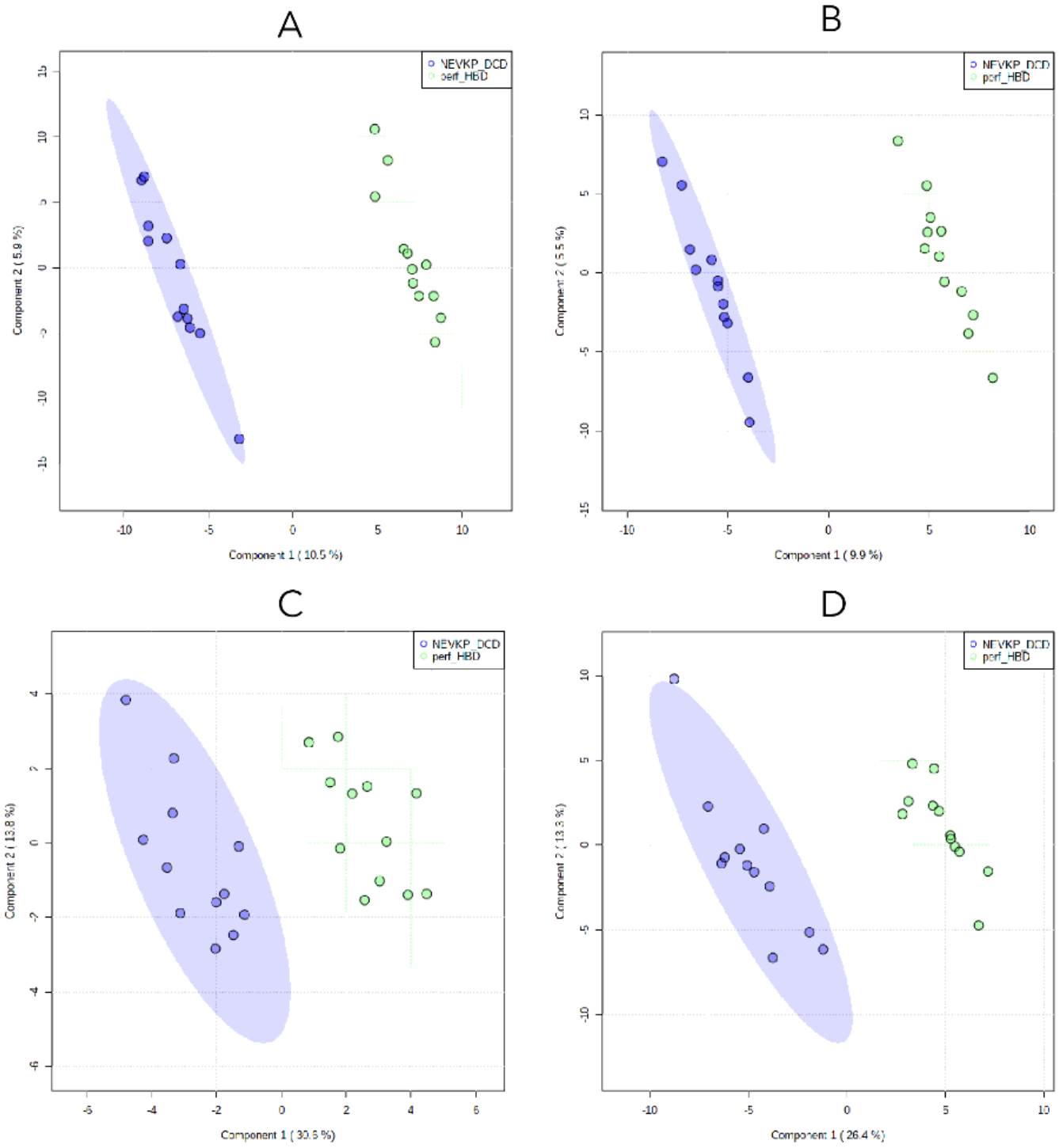

Figure 2

PLS-DA score plots showing the separation between HBD and DCD perfusions. RP metabolomic analyses in (A) positive and (B) negative ionization modes; lipidomic analyses with (C) HILIC and (D) RP

separations. For the metabolomic analyses, the Q2 and R2 values for the PLS-DA model were 73% and 96% for positive ionization mode and 71% and 96% for negative ionization mode, respectively. For the lipidomic analyses, the Q2 and R2 values for the PLS-DA model were 85% and 96% for HILIC separation and 91% and 99% for RP separation, respectively.

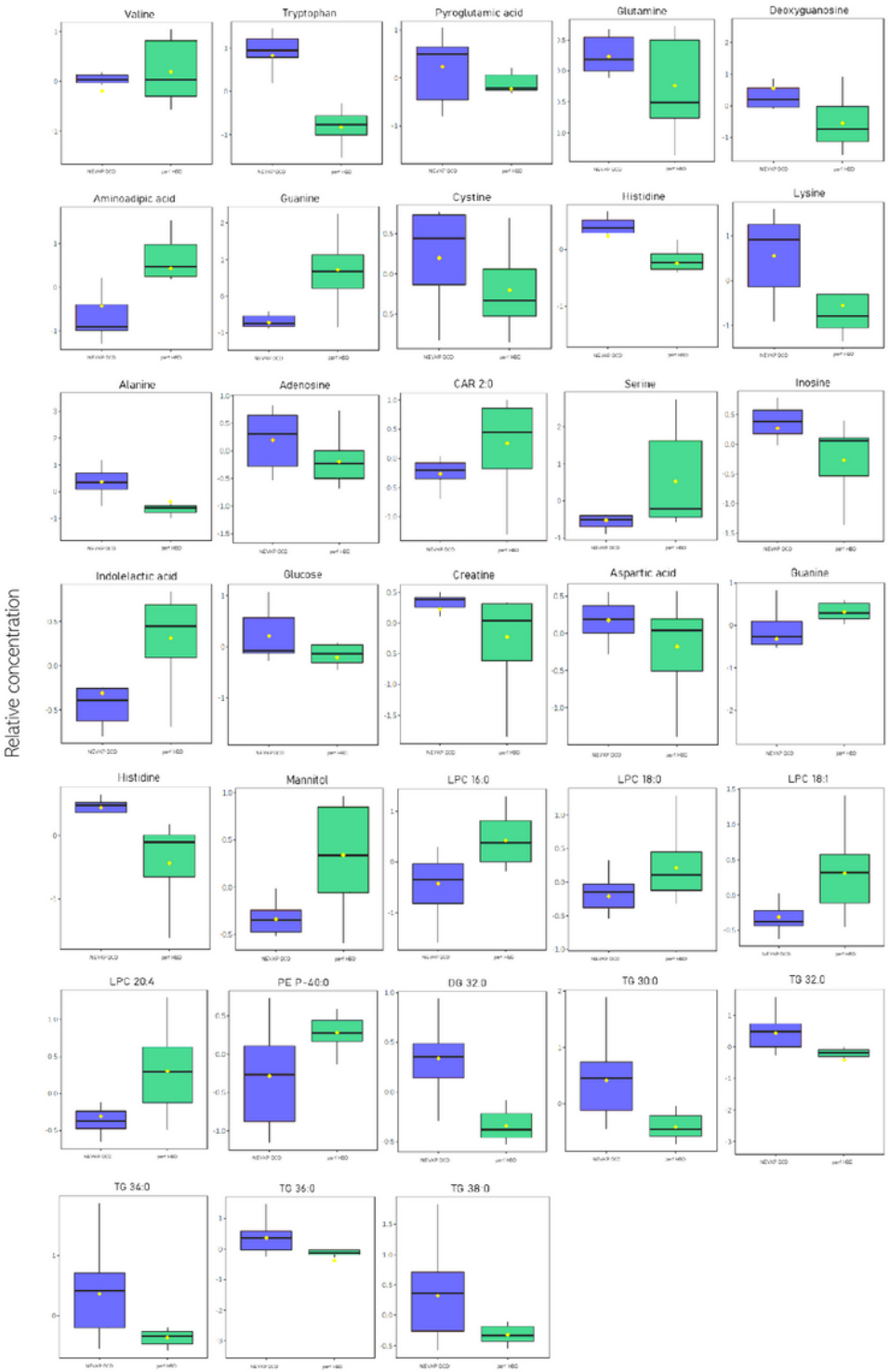

Figure 3

Levels of selected compounds detected between perfusions of HBD and DCD kidneys. The boxplots display normalized peak areas, with the notch indicating the 95% confidence interval around the median of each group. The mean concentration of each group is indicated with a yellow diamond.

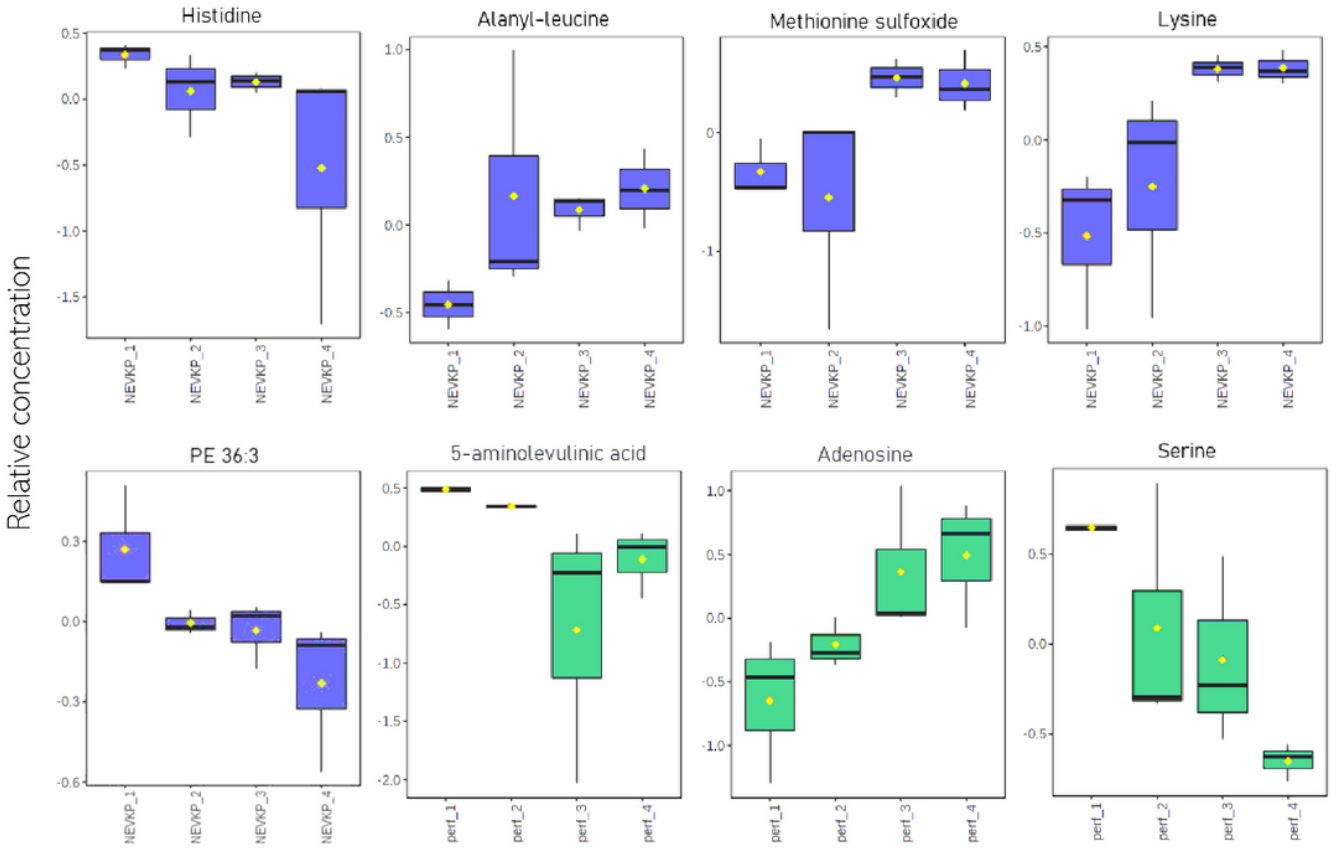

Figure 4

Linear correlations (r>0.7) between metabolites and time points across kidney perfusion. The boxplots display the normalized peak areas, while the notch indicates the 95% confidence interval around the median of each group. The mean concentration of each group is indicated with a yellow diamond.

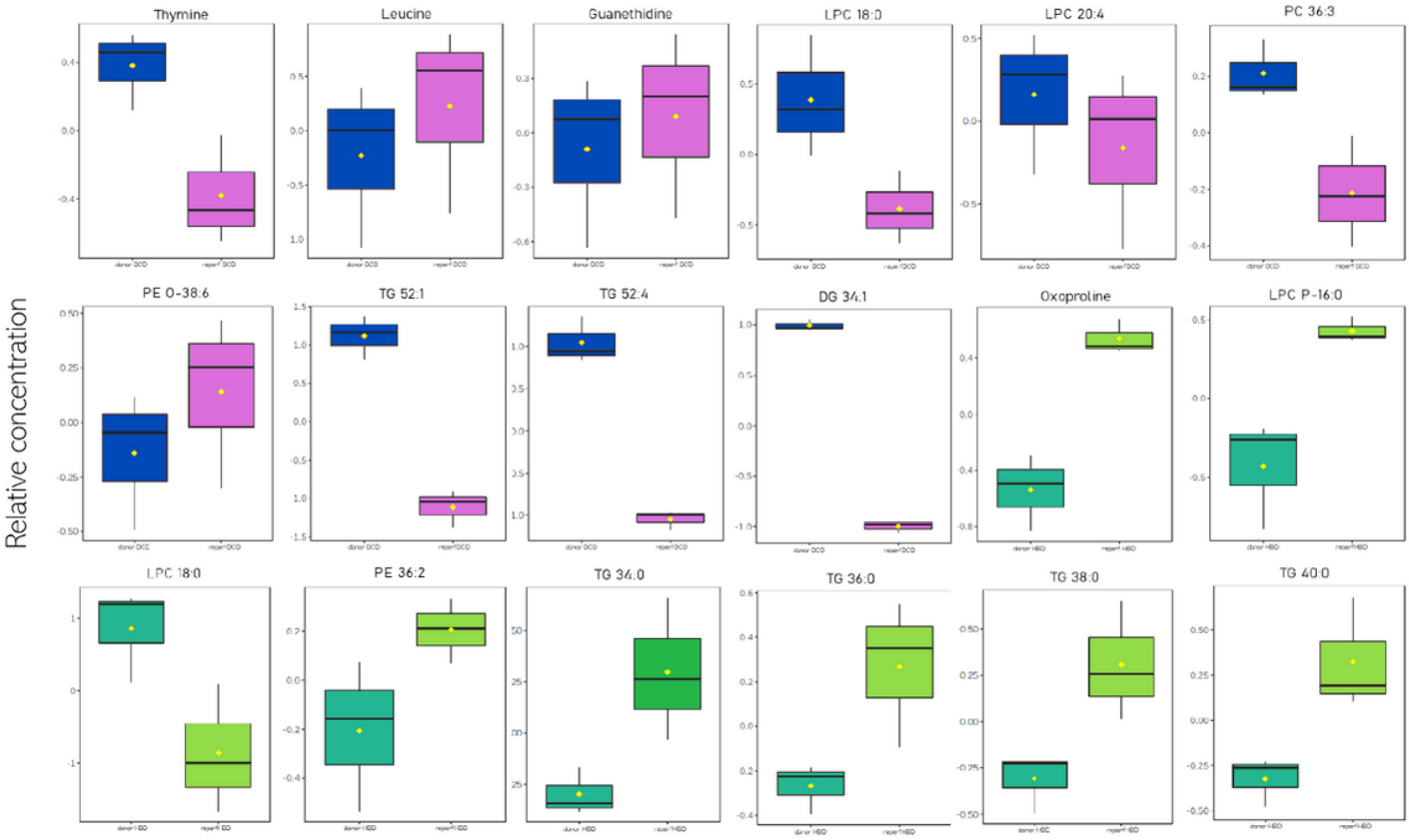

Figure 5

Change in the levels of selected compounds before and after the autotransplantation procedure. The boxplots display the normalized peak areas, while the notch indicates the 95% confidence interval around the median of each group. The mean concentration of each group is indicated with a yellow diamond.

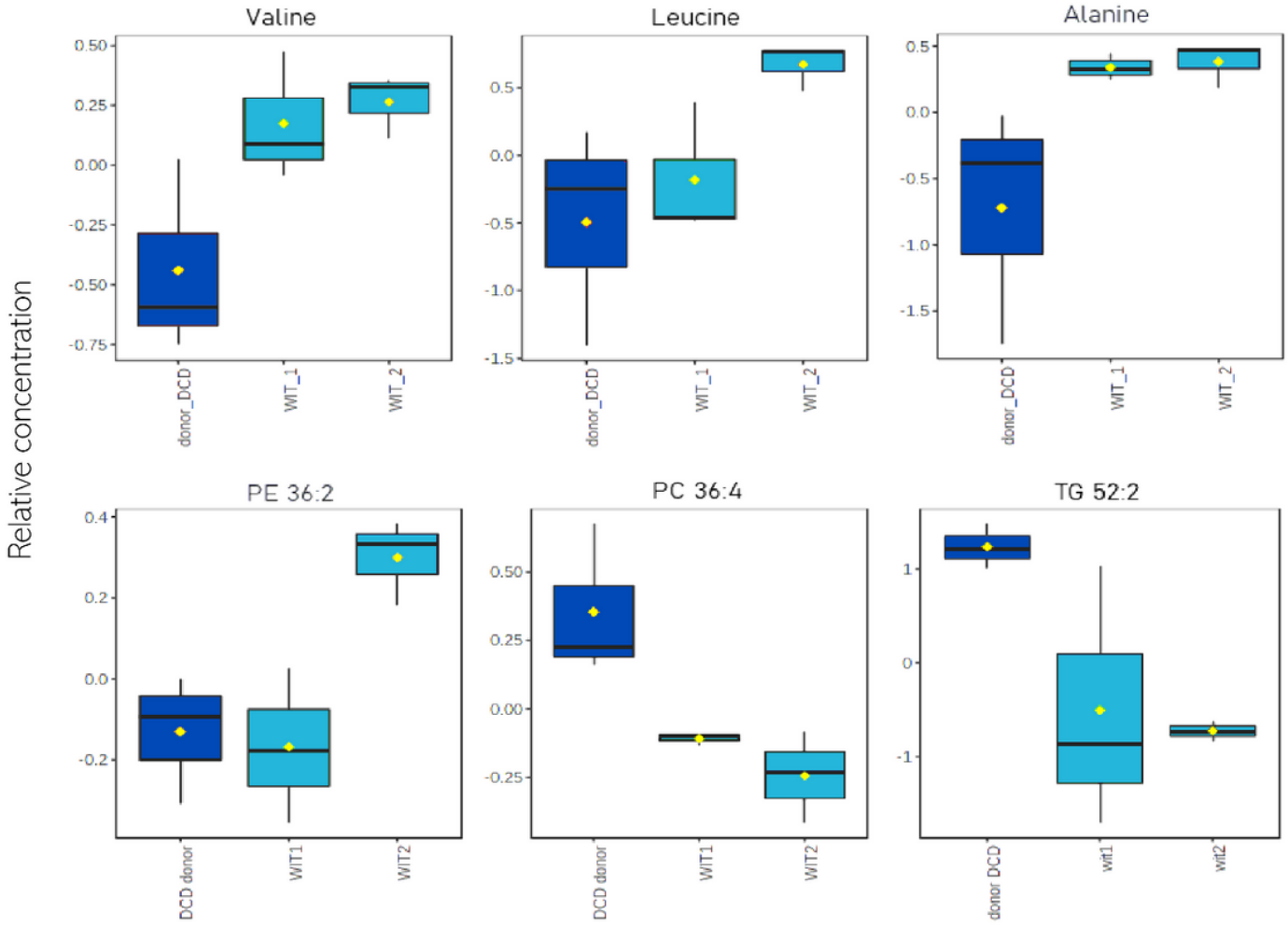

Figure 6

Linear correlations (r>0.7) between metabolites and time points across warm ischemia time. The boxplots display the normalized peak areas, while the notch indicates the 95% confidence interval around the median of each group. The mean concentration of each group is indicated with a yellow diamond.

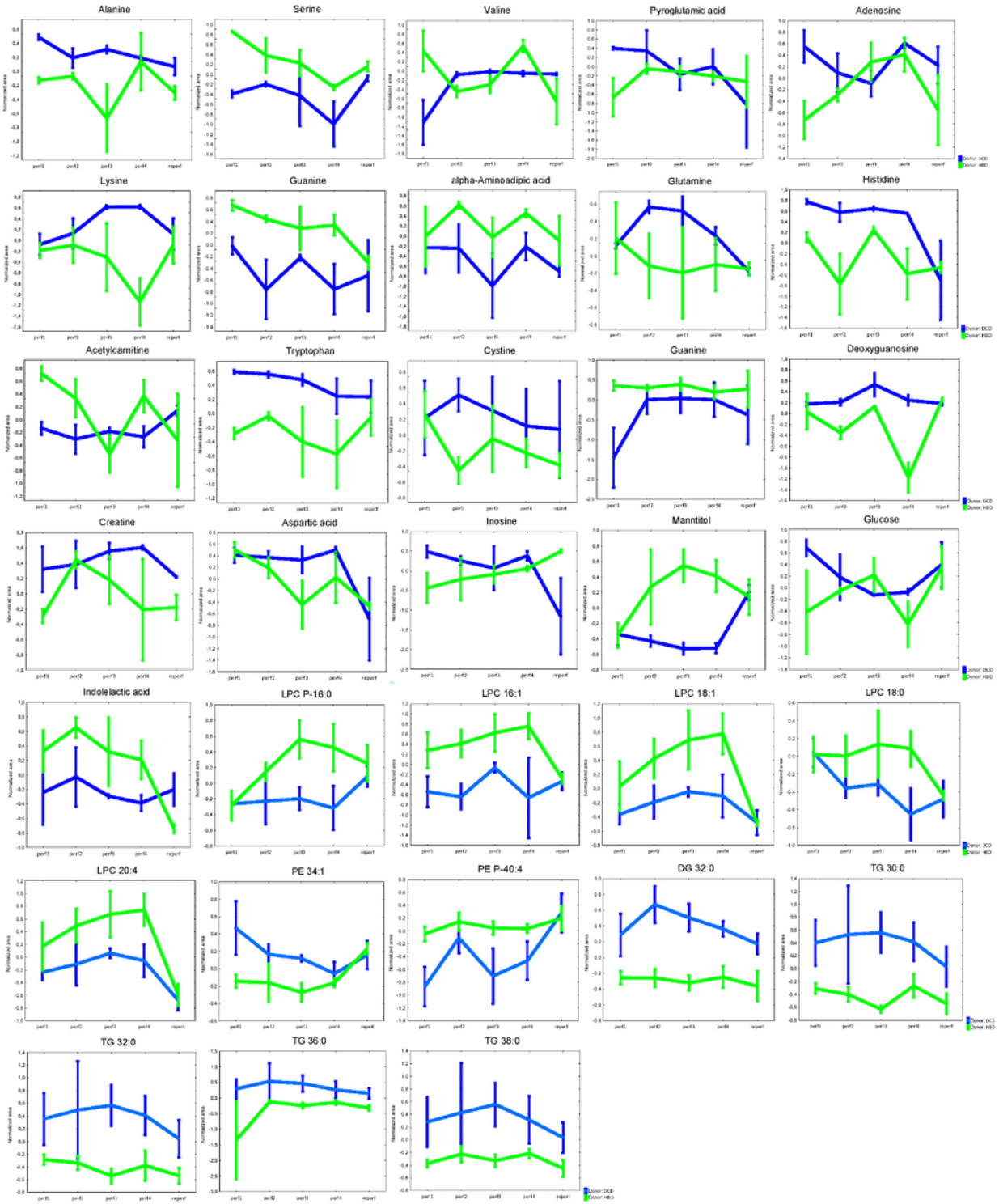

Figure 7

Change in levels of selected compounds differentiating perfusions across perfusion and reperfusion time points. The values are presented as mean ± SEM. Blue squares—DCD donors; green squares—HBD donors.

Supplementary Files

This is a list of supplementary files associated with this preprint. Click to download.

- SciRepSupplementaryMaterial.pdf
- graphicalabstract.tif